

Density Functional Study on the Adsorption of Pyrazole onto Silver Colloidal Particles

Gianni Cardini and Maurizio Muniz-Miranda*

Dipartimento di Chimica, Universita' di Firenze, Via della Lastruccia 3, I-50019 Sesto Fiorentino, Italy, and European Laboratory for Nonlinear Spectroscopy (LENS), Polo Scientifico, I-50019 Sesto Fiorentino, Italy

Received: November 14, 2001; In Final Form: February 22, 2002

The adsorption of pyrazole onto silver colloids has been investigated by surface-enhanced Raman scattering (SERS) experiments for normal and deuterated ligand and by *ab initio* density functional theory (DFT) calculations performed for surface complex models. The best agreement between observed and calculated frequencies occurs when the pyrazolide anion is bound to two partially charged Ag atoms of the colloidal surface. The formation of the adsorbate is closely related to the presence of adsorbed hydroxide anions, which are able to promote the deprotonation of the organic ligand.

1. Introduction

Surface-enhanced Raman scattering (SERS) represents a highly efficient technique to study the adsorption of ligands onto coinage metal surfaces (Ag, Au, and Cu) because the corresponding Raman signal is hugely enhanced, by many orders of magnitude, with respect to that of the nonadsorbed molecules. This is due both to the local electric field, intensified by the metal surface, and to the ligand electronic structure, modified by the chemical interaction with the substrate. Actually, by the large amount of experimental efforts, it is now well-established that an effective SERS enhancement is detected when the ligand is able to form a chemical bond with the surface or when a significant metal–molecule charge transfer occurs. The frequency shifts, observed in the SERS with respect to the normal Raman bands, play a significant role for investigating the adsorption mechanism because they are closely related to the atoms directly bound to the surface. On this basis, in the present work, we want to show how a comparison between *ab initio* calculations, performed on molecule–metal model systems, and experimental SERS results allows determination of the type and the structure of the adsorbate formed on the metal substrate.

Recently, the SERS spectrum of pyrazole in silver hydrosol¹ was attributed to the pyrazolide anion formed by deprotonation of the N–H group, when the molecule interacted with the silver surface. To confirm this hypothesis, new experimental data along with *ab initio* calculations are here reported. The SERS spectrum of the ligand is compared with that of the corresponding deuterio derivative and with the Raman spectrum of the silver(I)–pyrazolide coordination compound.

Because positively charged silver atoms can be present on the colloidal surface,² calculations on pyrazole and pyrazolide bound to silver atoms or cations have been performed to identify the most probable species adsorbed on the metal surface. Some insights on the adsorption mechanism and on the electronic density distribution of the adsorbate are also reported.

2. Experimental Section

Pyrazole (Aldrich, purity >99%), twice purified by sublimation under vacuum, was added (10^{-3} M concentration) to silver

hydrosols, prepared according to Creighton's procedure,³ aged a week to prevent the formation of reduction products.⁴ The resulting pH value of the colloidal dispersions was ~ 9 .

Perdeuteration of pyrazole was obtained by repeated reactions with K_2CO_3 in heavy water solution at about 200 °C.⁵ Silver(I)–pyrazolide complex was obtained by mixing pyrazole with $AgNO_3$ in aqueous solution with NH_3 , according to the old preparation by Buchner.⁶

Raman measurements were performed by using a Jobin-Yvon HG-2S monochromator, a cooled RCA-C31034A photomultiplier, and the 514.5 nm exciting line supplied by an Ar^+ laser with a power of 50 mW. The Raman spectrum of the argentous coordination compound was obtained by using a defocused laser beam and a rotating device to impair thermal effects.

3. Calculation Method

All *ab initio* calculations have been performed with the Gaussian 98 package⁷ using the combination of the B3LYP exchange correlation functional along with the Lanl2DZ basis set. In the case of pyrazole and pyrazolide, the density functional theory (DFT) calculations have been performed at the B3LYP/6-31++G(d,p) level of theory. The structures were optimized with a *tight* criterion, and the harmonic frequencies were calculated by using an improved grid in the calculation of the integrals (Integral(Grid = 199 974)). A uniform scaling factor of 0.9833 has been adopted for all the computed wavenumbers corresponding to the vibrational normal modes, as recently done by Aroca et al.⁸ for phthalimide adsorbed on silver.

4. Results

4.1. SERS Spectra. The SERS spectra of normal and deuterated pyrazole in silver hydrosol are compared in Figures 1 and 2 with the normal Raman spectra in water solution for different pH values. In aqueous solution at pH = 7, the neutral molecule represents the largely predominant form, while in highly alkaline medium (pH ≈ 14), the Raman spectrum of the pyrazolide anion is observed. The strong SERS band at 1129 cm^{-1} is closely related to the most intense Raman band of pyrazolide at about the same wavenumber (Figure 1). Also, the CH stretching bands in the SERS correspond to those observed in the normal Raman spectrum of the alkaline solution. In the case of deuterated samples (Figure 2), the strong Raman band

* To whom correspondence should be addressed. E-mail: muniz@chim.unifi.it.

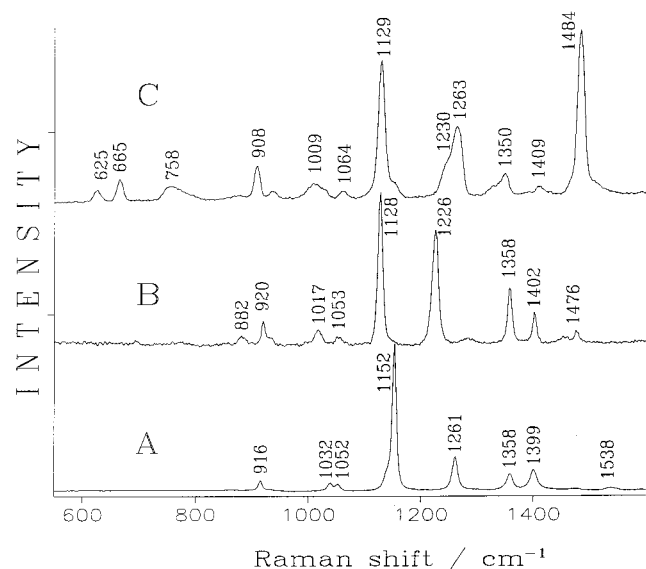


Figure 1. Raman spectra of pyrazole (A) and pyrazolide (B) in aqueous solutions compared with the SERS (C) of the ligand adsorbed on silver colloid.

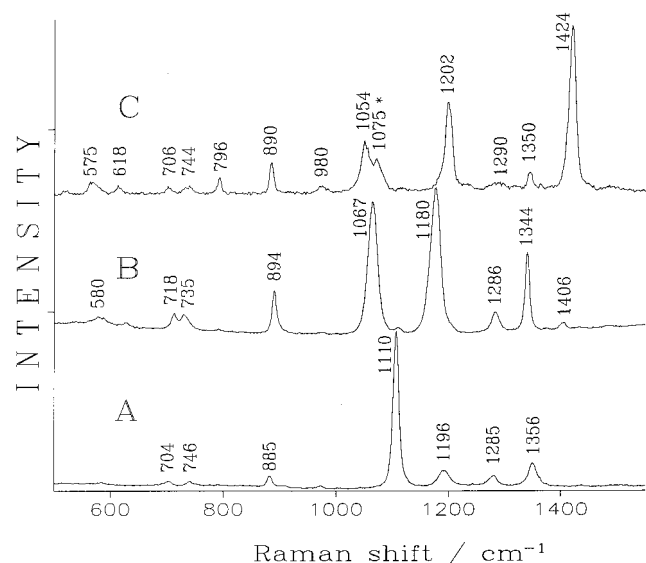


Figure 2. Raman spectra of pyrazole- d_3 (A) and pyrazolide- d_3 (B) in aqueous solutions compared with the SERS (C) of the deuterated ligand adsorbed on silver colloid. Dot refers to a carbonate ion band.

of pyrazole at 1110 cm^{-1} finds no counterpart in the SERS, while the SERS band at 1424 cm^{-1} corresponds to the Raman mode of deuterated pyrazolide at 1406 cm^{-1} .

The Raman spectrum of the silver(I)–pyrazolide coordination compound is reported in Figure 3. The presence of two Raman bands at 218 and 248 cm^{-1} , attributable to two Ag–N stretching modes, confirms the bidentate structure of the ligand in a polymeric arrangement.⁹ Moreover, the Raman bands at 1140 and 1484 cm^{-1} can be related to the SERS bands observed at 1129 and 1484 cm^{-1} (Figure 1). This evidence points to the presence of the pyrazolide anion on the silver surface as well as in the coordination compound. But observing the frequency differences between SERS and Raman spectrum of silver(I)–pyrazolide, it is questionable that this anion is really bound to two Ag^+ ions of the metal surface, as, instead, occurs in the silver(I)–pyrazolide complex.

4.2. DFT Calculations of Pyrazole and Pyrazolide. It has been widely shown that DFT is the most efficient correlated ab initio method to predict, with a high degree of accuracy, the

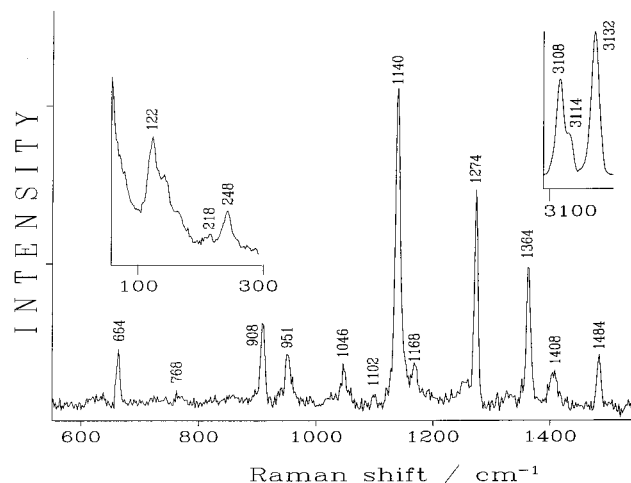
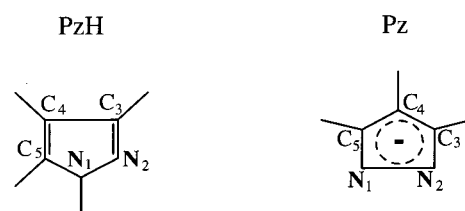


Figure 3. Raman spectrum of the silver(I)–pyrazolide coordination compound.



	a	b		a	b
N–N	1.351	1.383	N–N	1.365	1.399
N ₂ –C ₃	1.334	1.356	N–C	1.353	1.379
N ₁ –C ₅	1.360	1.377	C–C	1.407	1.420
C ₃ –C ₄	1.416	1.428			
C ₄ –C ₅	1.383	1.396			
N ₁ –H	1.008	1.010			
C ₃ –H	1.081	1.080	C ₃ –H, C ₅ –H	1.087	1.086
C ₄ –H	1.080	1.079	C ₄ –H	1.085	1.085
C ₅ –H	1.080	1.080			
N ₁ –N ₂ –C ₃	104.49	103.96	N–N–C	107.86	107.44
N ₂ –N ₁ –C ₅	113.21	112.76			
N ₂ –C ₃ –C ₄	111.91	111.78	N–C–C	110.91	110.94
N ₁ –C ₅ –C ₄	106.16	106.32			
C ₃ –C ₄ –C ₅	104.54	105.17	C–C–C	102.46	103.23
C ₄ –C ₃ –H	128.59	128.79			
C ₃ –C ₄ –H	128.20	127.68	C–C ₄ –H	128.77	128.38
C ₄ –C ₅ –H	131.92	131.22	C ₄ –C–H	128.81	128.93
N ₂ –N ₁ –H	118.91	118.63			

Figure 4. Optimized structures of pyrazole (PzH) and pyrazolide (Pz): (a) B3LYP/6-31++G(d,p); (b) B3LYP/Lanl2DZ. Bond distances are given in Å; bond angles are given in deg.

vibrational properties of medium and large molecules.¹⁰ In particular, the B3LYP along with the 6-31G(d) basis represents a quite satisfactory compromise between accuracy and computer requirements.^{11,12} Because the 6-31G(d) basis is not available for silver, we have adopted this functional along with the Lanl2DZ basis set, which makes use of ECP pseudopotentials for the silver atoms. To test the accuracy, we have obtained the equilibrium structures and the harmonic frequencies for pyrazole and pyrazolide with this basis and with the more commonly adopted 6-31++G(d,p) basis set. Both methods correctly predict the antiaromatic character (4π electrons) of pyrazole and the higher electronic delocalization of the pyrazolide anion. The structural data, reported in Figure 4, show a good agreement with the microwave spectral data of pyrazole.¹³ Moreover, the DFT calculations show the effect of the electronic delocalization in the pyrazolide anion, giving rise to bond lengths (N–C, 1.353 Å; C–C, 1.407 Å) as well as in heteroaromatic compounds. In

TABLE 1: Observed and Calculated Frequencies of Pyrazole (PzH) and Pyrazolide (Pz)

PzH			Pz		
obsd ^a	calcd ^b	calcd ^c	obsd ^d	calcd ^b	calcd ^c
3523	3618	3642			
3154	3231	3264	3122	3155	3186
3136	3214	3241	3090	3116	3147
3126	3202	3232		3111	3139
1531	1544	1525			
1447	1460	1428	1476	1458	1429
1394	1408	1391	1402	1391	1384
1357	1367	1351	1358	1351	1308
1254	1263	1252	1226	1201	1168
1159	1161	1145	1128	1152	1129
1121	1128	1123		1116	1097
1054	1041	1045	1053	1018	1021
1009	1033	1008	1017	1015	967
924	922	918	920	910	914
908	904	908	882	896	901
878	878	909		781	812
833	827	856	777	760	758
745	740	769	694	684	728
674	674	668		683	673
623	621	633		622	643
516	515	599			

^a Infrared data, vapor phase.²⁰ ^b B3LYP/6-31++G(d,p). ^c B3LYP/Lanl2DZ. ^d Raman data in aqueous solution.

contrast, in pyrazole, the N₂–C₃ (1.334 Å) and C₄–C₅ (1.383 Å) bond distances are closer to those typical of double bonds.

The frequencies, reported in Table 1, satisfactorily reproduce the experimental vibrational data, and the calculation method, performed with the Lanl2DZ basis set, shows sufficiently predictive properties for the subsequent studies. In particular, evidence of a correct spectral behavior is given by the trend of the C–H stretching frequencies, which show the expected decrease going from pyrazole to the pyrazolide anion, reaching values close to those typical of the aromatic systems (3050–3100 cm⁻¹). It can also be noted that the adopted scaling factor in this region is not sufficient to give a good agreement with the experimental data and should be further reduced in this spectral region. This is mainly due to the higher anharmonicity of these vibrations; anyway, we did not find it necessary for our aim to change the scaling factor, maintaining the same value for all the normal modes.

4.3. DFT Calculations on Models of Surface Complexes.

The calculated frequencies of pyrazole–silver and pyrazolide–silver complex models are reported in Tables 2 and 3, respectively, involving one or two silver atoms or ions, in comparison with the experimental ones. The aim of these calculations is to identify the species really adsorbed on silver by the best agreement with the SERS bands but not to reproduce the intensities. Actually, on the basis of the electromagnetic mechanism, the SERS intensities are dependent on the resonance between the frequency of the plasmon wave of the metal particles, where the ligand is adsorbed, and that of the exciting radiation. But the simple model system constituted by a ligand bound to one or two silver atoms (or ions) cannot take into account the plasmon waves localized onto the metal surface. Moreover, the SERS intensities are also dependent on the aqueous environment, where the presence of different ions can induce changes in the adsorption geometry;¹⁴ thus, they cannot be correctly reproduced by calculations performed in a vacuum. Finally, the SERS intensities can undergo resonance effects due to charge transfer between the energy levels of ligand and metal.¹⁵

These calculations seem to exclude the possibility that the SERS spectrum is due to pyrazole adsorbed on the metal surface

TABLE 2: Calculated Frequencies of Pyrazole/Silver Model Systems Compared with the SERS Data

PzHAg ⁺	PzHAg ^o	SERS
3620	3623	
3279	3279	3125
3254	3247	3124
3248	3239	3091
1527	1525	
1464	1428	1484
1408	1397	1409
1352	1352	1350
1277	1262	1263
1151	1146	
1141	1129	1129
1082	1054	1064
1045	1017	1009
948	928	
942	917	
909	912	908
892	867	
797	775	758
645	671	665
615	637	625
578	609	
215	89	235
151	64	
96	45	

TABLE 3: Calculated Frequencies of Pyrazolide/Silver Model Systems Compared with the SERS Data and the Raman Frequencies of the Silver(I)–Pyrazolide Complex

PzAg ^o	PzAg ⁺	PzAg ^o Ag ⁺	PzAg ^o Ag ^o	PzAg ⁺ Ag ⁺	SERS	complex
3215	3249	3252	3221	3269	3135	3132
3187	3222	3227	3193	3235	3124	3114
3174	3214	3219	3181	3233	3091	3108
1451	1471	1473	1458	1492	1484	1484
1394	1401	1413	1396	1432	1409	1408
1327	1333	1344	1333	1349	1350	1364
1206	1240	1261	1215	1261	1263	1274
1146	1152	1161	1150	1168		1168
1115	1128	1125	1122	1150	1129	1140
1041	1058	1072	1048	1092	1064	1102
989	988	999	1000	1041	1009	1046
919	914	942	924	963		951
914	912	917	916	923	908	
843	885	895	849	908		908
793	831	846	800	864		
738	753	762	741	778	758	768
665	645	647	666	621	665	664
638	613	628	637	621	625	
172	264	234	224	264	235	248
102	111	165	133	224		218
84	86	121	130	180		
		103	112	134		122
		90	34	54		
		78	34	53		

via a silver ion or a neutral silver atom (Table 2). In the first case, the surface complex, indicated as PzHAg⁺, can be ruled out by considering that the frequencies calculated at 797 and 1045 cm⁻¹ find no counterpart in the SERS. In the second complex, indicated as PzHAg^o, the Ag–N stretching mode occurs at a wavenumber (89 cm⁻¹) that is too low with respect to the SERS band observed at 235 cm⁻¹, almost like that in a physisorption process. This is also confirmed by scarce charge-transfer effect and Ag–N distance (2.514 Å) greater than the usual values found in the coordination compounds.

By assuming pyrazolide bound to the metal substrate (Table 3), the case of interaction with a single Ag atom can be easily excluded because the Ag–N stretching and the ring mode calculated at 172 and 1206 cm⁻¹, respectively, occur at wavenumbers that are too low with respect to the observed ones.

$\text{Pz Ag}^0\text{Ag}^+$

$\text{Pz Ag}^0\text{Ag}^0$

$\text{Pz Ag}^+\text{Ag}^+$

N-N	1.398	N-N	1.394	N-N	1.398
N-C	1.366	N ₁ -C ₅	1.377	N-C	1.371
		N ₂ -C ₃	1.369		
C-C	1.412	C ₅ -C ₄	1.409	C-C	1.405
		C ₃ -C ₄	1.422		
C ₃ -H ₃ /C ₅ -H	1.081	C ₃ -H	1.083	C ₃ -H ₃ /C ₅ -H	1.081
C ₄ -H	1.080	C ₄ -H	1.082	C ₄ -H	1.078
		C ₅ -H	1.083		
N-N-C	107.96	N ₁ -N ₂ -C ₃	106.20	N-N-C	107.67
		N ₂ -N ₁ -C ₅	109.27		
N-C-C	109.58	N ₁ -C ₅ -C ₄	109.33	N-C-C	109.81
		N ₂ -C ₃ -C ₄	111.22		
C-C-C	104.92	C-C-C	103.99	C-C-C	105.05
C-C ₄ -H	127.54	C ₅ -C ₄ -H	127.86	C-C ₄ -H	127.48
C ₄ -C-H	129.48	C ₄ -C ₃ -H	129.06	C ₄ -C-H	129.04
		C ₄ -C ₅ -H	129.77		
Ag-N	2.235	Ag-N ₁	2.177	Ag-N	2.123
Ag-N-N	108.77	Ag-N ₁ -N ₂	121.76	Ag-N-N	128.32
		Ag-N ₁ -C ₅	128.97		
Ag...Ag	2.836	Ag...Ag	2.667	Ag...Ag	4.031

Figure 5. Optimized structures of the surface complex models. Bond distances are given in Å; bond angles are given in deg.

TABLE 4: Mulliken Atomic Charges^a for the Surface Complexes Reported in Figure 5

atom	PzAg ⁺ Ag ⁰	PzAg ⁰ Ag ⁰	PzAg ⁺ Ag ⁺
N ₁	-0.207	-0.280	-0.288
N ₂	-0.207	-0.124	-0.288
C ₃	-0.215	-0.323	-0.104
C ₄	-0.298	-0.363	-0.275
C ₅	-0.215	-0.207	-0.104
H ₃	0.242	0.214	0.262
H ₄	0.246	0.209	0.282
H ₅	0.242	0.213	0.262
Ag ₁	0.206	-0.322	0.627
Ag ₂	0.206	-0.017	0.627

^a Elementary charge, $e = 1.602 \times 10^{-19}$ C.

The surface complex formed by pyrazolide bound to two Ag atoms and indicated as PzAg^0Ag^0 cannot also be taken into account by considering the low wavenumber of the ring mode calculated at 1215 cm^{-1} and the optimized structure (Figure 5), excluding a direct interaction of two silver atoms with the ligand. Among the remaining three surface complexes, the best agreement is obtained for the bidentate complex, formally indicated as PzAg^+Ag^0 , with pyrazolide bound to two silver atoms with a partially positive charge. The other bidentate complex, PzAg^+Ag^+ , instead, can be considered as a model for the silver(I)–pyrazolide coordination compound, of which the Raman bands are sufficiently well-reproduced (Table 3). In particular, the DFT calculations predict two Ag–N stretching modes at 224 and 264 cm^{-1} , very close to the corresponding Raman bands observed at ~ 220 and 250 cm^{-1} .

The optimized structures of the three possible surface complexes with two silver atoms or ions are reported in Figure 5. By considering the Mulliken atomic charges, as reported in Table 4, it is possible to remark that the charge transfer from the ligand to the metal is more effective when the complex is neutral (PzAg^+Ag^0) or positively charged (PzAg^+Ag^+), with -0.59 or -0.75 elementary charge (e), respectively, transferred

TABLE 5: Observed and Calculated Frequencies of Deuterated Pyrazolide (Pzd_3) in Comparison with the Calculated Frequencies of the Surface Complex Models and the SERS Data

Pzd ₃ obsd ^a	Pzd ₃ calcd ^b	Pzd ₃ Ag ⁺	Pzd ₃ Ag ⁰ Ag ⁺	Pzd ₃ Ag ⁺ Ag ⁺	SERS
2350	2376	2425	2427	2440	2359
2310	2330	2387	2393	2401	2325
2204	2315	2373	2378	2391	2310
1406	1352	1407	1410	1427	1424
1344	1330	1343	1354	1376	1350
1286	1229	1264	1281	1274	1290
1180	1129	1179	1197	1197	1202
1067	1026	1054	1058	1100	1054
976	964	956	981	1002	980
894	886	914	923	934	924
		889	894	892	890
794	767	780	789	804	796
735	714	758	767	785	
718	712	739	744	757	744
	678	687	706	716	706
592	578	585	596	593	618
580	555	573	579	575	575
536	517	517	520	515	522
		259	230	259	246
		107	158	221	
		83	118	169	
			103	130	
			87	53	
			73	30	

^a Raman data in aqueous solution. ^b B3LYP/6-31++G(d,p).

from pyrazolide to the substrate, against $-0.39e$ in the case of the negative complex (PzAg^0Ag^0). In the surface complex PzAg^+Ag^0 , a strong negative charge is quite uniformly delocalized all over the ring, with positively charged hydrogen atoms. The Ag–Ag distance for the complex PzAg^+Ag^+ is very large ($> 4\text{ Å}$), while in the complex PzAg^+Ag^0 , it corresponds to the distance observed in the silver crystal (2.84 Å), improving the hypothesis that this is the species really present on the metal substrate.

A further confirmation derives from DFT calculations on deuterated complexes, in virtue of the best agreement with the experiments (Table 5). This is particularly evident in the regions around 1000 and 1350 cm^{-1} . In Table 6, the vibrational assignment for the complex PzAg^+Ag^0 , as deriving from the calculated Cartesian displacements, is reported along with the experimental frequencies for normal and deuterated ligands. All of the bands observed in the SERS spectra correspond to in-plane vibrations; the intense bands, detected at 908 , 1009 , 1129 , 1263 , and 1484 cm^{-1} and at 796 , 890 , 1054 , 1202 , and 1424 cm^{-1} for the normal and deuterated compounds, respectively, correspond to totally symmetric ring deformation modes. It is interesting to note that the ring vibration at the highest frequency occurs along the direction of the ligand \rightarrow metal charge transfer (Figure 6). In agreement with the surface selection rules for photoassisted charge-transfer effect,¹⁶ this band is the most intense in the SERS spectrum. The broad band observed at about 240 cm^{-1} in the SERS of normal or deuterated pyrazole, attributable to the symmetric Ag–N stretching mode, can be described, instead, as translation of the ligand with respect to the substrate, as proposed in the case of 2,2'-bipyrimidine adsorbed on silver.¹⁷ Finally, as correctly found in the calculations, the CH or CD stretching modes undergo upshift upon adsorption.

4.4. Adsorption Mechanism. As a consequence of the DFT calculations reported above, a reasonable adsorption mechanism of pyrazole, involving the formation of the surface complex

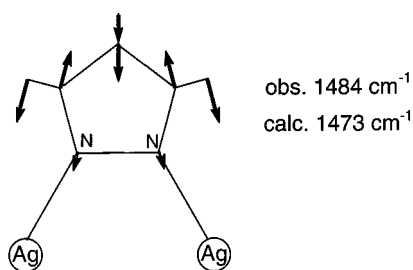


Figure 6. Cartesian displacements for the ring stretching vibration observed at 1484 cm^{-1} .

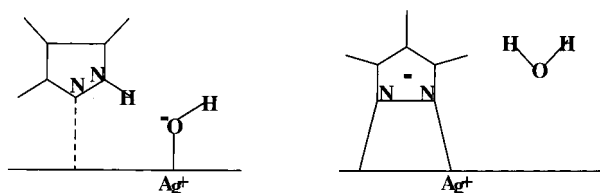


Figure 7. Adsorption mechanism of pyrazole onto the silver colloidal surface.

TABLE 6: Assignment of the SERS Frequencies of the Normal and Deuterated Ligands

species	normal		deuterated		assignment
	obsd	calcd	obsd	calcd	
A ₂		78		73	op ring rotation
B ₂		90		87	op ring rotation
A ₁		103		103	Ag–Ag stretching
B ₁		121		118	asym Ag–N stretching
B ₁		165		158	ip ring rotation
A ₁	235	234	246	230	sym Ag–N stretching
B ₂	625	628	522	520	op ring deformation
A ₂	665	647	618	596	op ring deformation
B ₂	758	762	575	579	C–H wagging
A ₂		846	706	706	C–H wagging
B ₂		895		767	C–H wagging
A ₁	908	917	796	789	ip ring deformation
B ₁		942	744	744	ip ring deformation
A ₁	1009	999	890	894	ip C–H bending + N–N stretching
B ₁	1064	1072	924	923	ip C–H bending
A ₁	1129	1125	1054	1058	ring breathing
B ₁		1161	980	981	ip C–H bending + ring deformation
A ₁	1263	1261	1202	1197	N–N stretching
B ₁	1350	1344	1290	1281	ring deformation + ip C–H bending
B ₁	1409	1413	1350	1354	ring deformation + ip C–H bending
A ₁	1484	1473	1424	1410	C–N, C–C stretchings
A ₁	3091	3219	2310	2378	C–H stretching
B ₁	3124	3227	2325	2393	C–H stretching
A ₁	3135	3252	2359	2427	C–H stretching

$\text{PzAg}^+\text{Ag}^\circ$, can be proposed. First, the pyrazole molecule approaches the silver surface, interacting through the pyridinic nitrogen. Then, an acid–base reaction between an adsorbed OH^- ion and the hydrogen atom bound to the pyrrolic nitrogen occurs. Hence, the pyrazolide anion can interact with the surface Ag^+ cluster where the hydroxide ion was previously bonded (Figure 7).

The presence of hydroxide ions on the silver surface derives from the reduction of AgNO_3 with NaBH_4 in the preparation of the colloid,³ of which the aqueous solution is alkaline ($\text{pH} \approx 9$). The adsorption of these anions produces Ag atoms positively charged and able to bind an electron donor like the pyrazolide anion. A similar mechanism has been previously proposed¹⁸ for the adsorption of 2-amino-5-nitropyridine (ANP)

on silver colloid, for which the adsorbed species was the anion ANP^- . In that case, the SERS spectrum closely corresponded to the Raman spectrum of the complex $\text{Ag(I)}-\text{ANP}^-$. In the present case, instead, the pyrazolide anion is bound to two Ag atoms, one of which is formally charged, while the corresponding coordination compound presents a polymeric structure with pyrazolide bound to two Ag^+ ions at a bridge.⁹

When the OH^- ions are removed from the silver surface because of addition of an acid solution, the pyrazole molecule adsorbs on silver, giving rise to a different SERS spectrum¹ with experimental frequencies detected at 230, 615, 776, 935, 1150, 1273, 1354, 1435, and 1508 cm^{-1} . These bands are matched by the calculations reported in Table 2 for the complex PzHAg^+ , whereas the calculated frequencies for the complex PzHAg° do not agree with the experimental findings. In particular, the Ag–N stretching mode, detected at about 230 cm^{-1} in silver hydrosol at acidic pH, is not reproduced when pyrazole is assumed to interact with a neutral silver atom. As previously stated, the optimized structure for this complex shows a quite long Ag–N distance, suggesting the hypothesis of a quite weak chemisorption.

5. Conclusions

The SERS spectroscopy can represent a powerful tool to understand the adsorption mechanism, if properly supported by a theoretical interpretation. In the past, the interpretation of the SERS data was limited to normal-mode calculations performed on model systems deduced from the corresponding coordination compounds.^{14,17,19} Although this approach has been fruitful to reproduce the frequency shifts observed upon adsorption, a further improvement in the interpretation of the experimental data can be performed now by ab initio calculations mainly based on the density functional formalism. In the present paper, we have adopted the B3LYP functional to study a series of possible surface complexes and to obtain information on the adsorption mechanism of pyrazole on silver colloid. We have considered both pyrazole and pyrazolide bound to one or two Ag atoms assuming that each metal atom can be initially neutral or a cation. These calculations have allowed the proposal of the pyrazolide anion in a bidentate interaction with the silver surface as the species responsible for the observed SERS spectrum and evaluation of variations in the structure and in the atomic charge distribution. We have found that pyrazolide, when adsorbed on silver colloidal particles, exhibits charge delocalization upon the ring and transfers half of its negative charge to the metal. The formation of this adsorbate is closely related to the presence of hydroxide anions coadsorbed onto the silver surface.

Finally, because in the real situation the adsorption occurs on a silver surface and our calculation model is limited to consideration of an active site with one or two Ag atoms, we have performed, as a check, an additional calculation with three Ag atoms. Therefore, the $\text{Pz}(\text{Ag}_2)^+$ complex has been compared with the $\text{Pz}(\text{Ag}_3)^+$ complex at the same level of theory (B3LYP/LanL2DZ). We have not obtained significant differences on the optimized structure of the ligand, as well as on the calculated normal modes. The main effect of adding another silver atom into the metal ion cluster is limited to a small upshift of the vibrational modes involving the nitrogen atoms bound to silver. Additional calculations are in progress to take into account larger silver clusters as proposed by Roy and Furtak²¹ for the pyridine/silver complex to model also the SERS intensities.

Acknowledgment. The authors gratefully thank the Italian Ministero dell'Istruzione, Università e Ricerca (MIUR) and the

Consiglio Nazionale delle Ricerche (CNR) for the financial support to the "Progetto Finalizzato Materiali Speciali II".

References and Notes

- (1) Muniz-Miranda, M.; Neto, N.; Sbrana, G. *J. Mol. Struct.* **1999**, *482*, 207.
- (2) Muniz-Miranda, M.; Sbrana, G. *J. Raman Spectrosc.* **1996**, *27*, 105.
- (3) Creighton, J. A.; Blatchford, C. G.; Albrecht, M. G. *J. Chem. Soc., Faraday Trans. II* **1979**, *75*, 790.
- (4) Muniz-Miranda, M.; Neto, N.; Sbrana, G. *J. Mol. Struct.* **1986**, *143*, 275.
- (5) Frediani, P.; Rovai, D.; Muniz-Miranda, M.; Salvini, A.; Caporali, M. *Catal. Commun.* **2001**, *2*, 125.
- (6) Buchner, E. *Chem. Ber.* **1889**, *22*, 842.
- (7) Frisch, M. J.; Trucks, G. W.; Schlegel, H. B.; Scuseria, G. E.; Robb, M. A.; Cheeseman, J. R.; Zakrzewski, V. G.; Montgomery, J. A., Jr.; Stratmann, R. E.; Burant, J. C.; Dapprich, S.; Millam, J. M.; Daniels, A. D.; Kudin, K. N.; Strain, M. C.; Farkas, O.; Tomasi, J.; Barone, V.; Cossi, M.; Cammi, R.; Mennucci, B.; Pomelli, C.; Adamo, C.; Clifford, S.; Ochterski, J.; Petersson, G. A.; Ayala, P. Y.; Cui, Q.; Morokuma, K.; Malick, D. K.; Rabuck, A. D.; Raghavachari, K.; Foresman, J. B.; Cioslowski, J.; Ortiz, J. V.; Stefanov, B. B.; Liu, G.; Liashenko, A.; Piskorz, P.; Komaromi, I.; Gomperts, R.; Martin, R. L.; Fox, D. J.; Keith, T.; Al-Laham, M. A.; Peng, C. Y.; Nanayakkara, A.; Gonzalez, C.; Challacombe, M.; Gill, P. M. W.; Johnson, B. G.; Chen, W.; Wong, M. W.; Andres, J. L.; Head-Gordon, M.; Replogle, E. S.; Pople, J. A. *Gaussian 98*; Gaussian, Inc.: Pittsburgh, PA, 1998.
- (8) Aroca, R. F.; Clavijo, R. E.; Halls, M. D.; Schlegel, H. B. *J. Phys. Chem. A* **2000**, *104*, 9500.
- (9) Masciocchi, N.; Moret, M.; Cairati, P.; Sironi, A.; Ardizzola, G. A.; La Monica, G. *J. Am. Chem. Soc.* **1994**, *116*, 7668.
- (10) Schettino, V.; Gervasio, F. L.; Cardini, G.; Salvi, P. R. *J. Chem. Phys.* **1999**, *110*, 3241.
- (11) Rauhut, G.; Pulay, R. *J. Phys. Chem.* **1995**, *99*, 3093.
- (12) Scott, A. P.; Radom, L. *J. Phys. Chem.* **1996**, *100*, 16502.
- (13) Nygaard, L.; Christensen, D.; Nielsen, J. T.; Pedersen, E. J.; Snerling, O.; Verstergaard, E.; Sorensen, G. O. *J. Mol. Struct.* **1974**, *22*, 401.
- (14) Muniz-Miranda, M. *J. Phys. Chem. A* **2000**, *104*, 7803.
- (15) Srnová-Sloufová, I.; Vlcková, B.; Snoeck, T. L.; Stufkens, D. J.; Matejka, P. *Inorg. Chem.* **2000**, *39*, 3551.
- (16) Lombardi, J. R.; Birke, R. L.; Lu, T.; Xu, J. *J. Chem. Phys.* **1986**, *84*, 4174.
- (17) Sbrana, G.; Neto, N.; Muniz-Miranda, M.; Nocentini, M. *J. Phys. Chem.* **1990**, *94*, 3706.
- (18) Neto, N.; Muniz-Miranda, M.; Sbrana, G. *J. Mol. Struct.* **1995**, *348*, 261.
- (19) Neto, N.; Muniz-Miranda, M.; Sbrana, G. *J. Phys. Chem.* **1996**, *100*, 9911.
- (20) Majoube, M. *J. Raman Spectrosc.* **1989**, *20*, 49.
- (21) Roy, D.; Furtak, T. E. *Phys. Rev. B* **1986**, *34*, 5111.